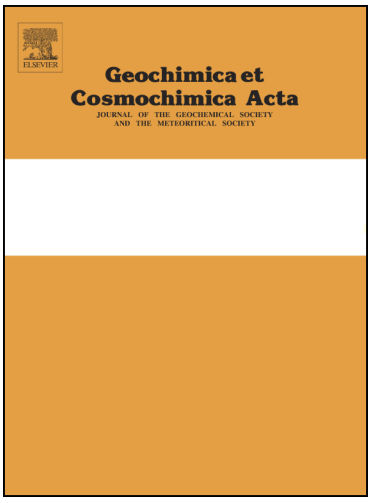

Juvenile crust formation in the Zimbabwe Craton deduced from the O-Hf isotopic record of 3.8-3.1 Ga detrital zircons

Robert Bolhar, Axel Hofmann, AnthonyI S. Kemp, Martin J. Whitehouse, Sandra Wind, Balz S. Kamber

PII: S0016-7037(17)30416-7
DOI: http://dx.doi.org/10.1016/j.gca.2017.07.008
Reference: GCA 10370

To appear in: *Geochimica et Cosmochimica Acta*

Received Date: 13 April 2016
Accepted Date: 6 July 2017

Please cite this article as: Bolhar, R., Hofmann, A., Kemp, A.S., Whitehouse, M.J., Wind, S., Kamber, B.S., Juvenile crust formation in the Zimbabwe Craton deduced from the O-Hf isotopic record of 3.8-3.1 Ga detrital zircons, *Geochimica et Cosmochimica Acta* (2017), doi: http://dx.doi.org/10.1016/j.gca.2017.07.008

Juvenile crust formation in the Zimbabwe Craton deduced from the O-Hf isotopic record of 3.8-3.1 Ga detrital zircons

Robert Bolhar[1,2)✉], Axel Hofmann[3)], Anthony I. S. Kemp[4)], Martin J. Whitehouse[5)], Sandra Wind[3,6)] and Balz S. Kamber[7)]

1) School of Geosciences, University of the Witwatersrand, Johannesburg, South Africa

2) School of Environmental and Earth Sciences, University of Queensland, Brisbane, Australia

3) Department of Geology, University of Johannesburg, Johannesburg, South Africa

4) School of Earth Sciences, University of Western Australia, Perth, Australia

5) Department of Geosciences, Swedish Museum of Natural History, Stockholm, Sweden

6) Institut für Geowissenschaften, Universität Kiel, Kiel, Germany

7) School of Natural Sciences, Trinity College Dublin, Dublin , Ireland

ABSTRACT

Hafnium and oxygen isotopic compositions measured in-situ on U-Pb dated zircon from Archaean sedimentary successions belonging to the 2.9-2.8 Ga Belingwean/Bulawayan groups and previously undated Sebakwian Group are used to characterize the crustal evolution of the Zimbabwe Craton prior to 3.0 Ga. Microstructural and compositional criteria were used to minimize effects arising from Pb loss due to metamorphic overprinting and interaction with low-temperature fluids. $^{207}Pb/^{206}Pb$ age spectra (concordance > 90%) reveal prominent peaks at 3.8, 3.6, 3.5, and 3.35 Ga, corresponding to documented geological events, both globally and within the Zimbabwe Craton. Zircon $\delta^{18}O$ values from +4 to +10 ‰ point to both derivation from magmas in equilibrium with mantle oxygen and the incorporation of

✉ corresponding author: email: robert.bolhar@wits.ac.za

material that had previously interacted with water in near-surface environments. In ε_{Hf}-time space, 3.8-3.6 Ga grains define an array consistent with reworking of a mafic reservoir ($^{176}Lu/^{177}Hf$ ~0.015) that separated from chondritic mantle at ~3.9 Ga. Crustal domains formed after 3.6 Ga depict a more complex evolution, involving contribution from chondritic mantle sources and, to a lesser extent, reworking of pre-existing crust. Protracted remelting was not accompanied by significant mantle depletion prior to 3.35 Ga. This implies that early crust production in the Zimbabwe Craton did not cause complementary enriched and depleted reservoirs that were tapped by later magmas, possibly because the volume of crust extracted and stabilised was too small to influence mantle isotopic evolution. Growth of continental crust through pulsed emplacement of juvenile (chondritic mantle-derived) melts, into and onto the existing cratonic nucleus, also involved formation of complementary depleted subcontinental lithospheric mantle since the early Archaean, indicative of strongly coupled evolutionary histories of both reservoirs, with limited evidence for recycling and lateral accretion of arc-related crustal blocks until 3.35 Ga.

Keywords: *Archaean, detrital zircon, greenstone belts, U/Pb-O-Hf isotopes, Zimbabwe Craton*

1. Introduction

The discovery of detrital zircon of Hadean age (> 4 Ga) in sedimentary rocks of the Yilgarn Craton has stimulated much research on the time-period for which virtually no rock record exists. Regardless of the opposing opinions about the origin of Hadean zircons - ranging from felsic magmatism at plate boundaries on a cool, wet early Earth, crystallisation in impact-generated melt pools, to re-melting of an originally

mafic proto-crust (e.g. Amelin et al., 1999; Wilde et al., 2001; Cavosie et al., 2005; Blichert-Toft and Albarede, 2008; Kemp et al., 2010; Guitreau et al., 2012; Zeh et al., 2014; Reimink et al., 2016; Kenny et al., 2016; Bauer et al., 2017) - there is consensus that the discovery of more locations with Hadean and early Archaean zircons and rocks would be highly desirable. The Yilgarn Craton has yielded Hadean zircon from several supracrustal rock successions (e.g. Froude et al., 1983; Wilde et al., 2001; Wyche et al., 2004; Nemchin et al., 2006) despite the fact that its rock record does not go beyond ca. 3.73 Ga (Kinny et al., 1988). A natural place to search for ancient terrestrial zircon is the Zimbabwe Craton, as it is believed to have shared at least some of its Archean history with the Yilgarn Craton, prompting the notion of the 'Zimgarn' Supercraton (Smirnov et al., 2013).

The geology of the Zimbabwe Craton is not well studied with modern geochronological and isotopic methods but, along with the Yilgarn Craton and others (e.g. Wyoming, Slave), it has been classified as a so-called high-μ region (Oversby, 1975) because of its higher-than-mantle $^{238}U/^{204}Pb$ source characteristics of exposed rocks. Explanations for this signature include sediment recycling (Mueller and Wooden, 1988), intra-crustal differentiation (Kramers and Tolstikhin, 1997), or inheritance from >3.8 Ga crustal precursor material (Kamber et al., 2003), possibly from a long-lived, stable (basaltic) Hadean protocrust (Kamber et al., 2005).

Other evidence for the antiquity of the Zimbabwe Craton includes the extremely retarded Os isotope composition of chromites from Archean ultramafic intrusions, requiring the growth of subcontinental lithospheric mantle since at least 3.8 Ga (Nägler et al., 1997). The few existing detrital zircon studies have found grains dating back to exactly 3.80 - 3.81 Ga (Dodson et al., 1988). A study of mantle xenoliths, kimberlitic macrocrysts and sulfide inclusions in diamond has since

provided additional Os isotope and PGE evidence for cratonic lithosphere formation since at least 3.4 Ga (Smith et al., 2009). Existing age data thus point to a consistent evolutionary history of the craton, commencing as early as 3.8 to 4.0 Ga (Kamber, 2015). The protracted cratonic history was already beginning to emerge from whole rock Pb isotope studies of intrusive suites in Zimbabwe, in which high U/Pb sources were postulated to have been remobilized since Palaeoarchaean times (e.g. Moorbath et al., 1977; Taylor et al., 1991; Berger and Rollinson, 1997).

Regardless of the possible 'Zimgarn' connection, the extremely limited exposure of ancient rocks (>3.5 Ga, Nutman, 2013) means that a global assessment of craton formation relies on more isotopic studies of ancient detrital zircon, ideally from a sufficiently large number of representative cratonic regions.

In this context, the principal aims of this study were:

(i) to augment the presently limited U-Pb geochronological dataset for detrital zircon from the Zimbabwe Craton;

(ii) to increase the geographic coverage on the craton from where the detrital zircons were sampled relative to previous studies (e.g. Dodson et al., 1988; Nägler et al., 1997);

(iii) to undertake a search for the most ancient zircons preserved to better delineate the extent of the oldest parts of the craton ("Tokwe segment": Wilson et al., 1995; Horstwood et al., 1999);

(iv) to use coupled O-Hf isotopic data obtained from precisely dated and well-characterized zircon to constrain the source(s) from which the craton grew; and

(v) to compare and contrast the detrital zircon record on the Zimbabwe Craton with that of other cratonic areas.

2. Geology of the Zimbabwe Craton

The oldest part of the Zimbabwe Craton is the pre-3.35 Ga Sebakwe proto-craton of Horstwood et al. (1999), which includes high-grade gneiss terrains of the Tokwe segment east of the Belingwe-Shurugwi greenstone belts (e.g. Wilson et al., 1995) and the Rhodesdale granitoid-gneiss terrain east of the Midlands greenstone belt (Robertson, 1976) (Fig.1). The old gneiss terrains include banded, migmatitic varieties and homogeneous, foliated varieties of tonalitic to granitic composition. Different phases within the TTGs have been dated between c. 3.57 and 3.37 Ma (e.g. Horstwood et al. 1999). Gneisses from the Tokwe segment have Sm-Nd T_{DM} ages between 3.65 and 3.51 Ga (Horstwood et al., 1999; Taylor et al., 1991) and low initial Sr ratios (0.700–0.701; Hawkesworth et al., 1975; Moorbath et al., 1977), suggesting that they were derived from depleted or chondritic mantle sources. Numerous infolded greenstone remnants (several kilometres long) have been assigned to the undated Sebakwian Group. The gneisses are intruded by the 3.38 Ga (U-Pb SIMS, Dodson et al. 1988) Mushandike granite and the c. 3.35 Ga (Pb-Pb, Taylor et al., 1991) Mont d'Or 'granite', both of which are foliated but not banded (Fig. 1). These intrusions were regarded as post-kinematic with respect to the formation of the regional north-oriented fabric and intrusive into Sebakwian Group greenstones, thus providing a minimum age for the Sebakwian Group (Wilson, 1968). However, nowhere do the granites cut the supracrustal enclaves, calling the proposal by Wilson (1968) into question. U-Pb zircon ages of migmatites in the Tokwe segment have identified two distinct amphibolite facies metamorphic events at c. 3.35 and 2.86 Ga (Nägler et al., 1997; Horstwood et al., 1999), reflecting anatexis and crustal reworking.

Basement gneisses border a volcano-sedimentary succession containing intermediate to felsic volcanics and their volcaniclastic equivalents, komatiites and basalt with intercalations of banded iron formation and clastic sedimentary rocks (Fig. 1). These rocks have been assigned to the Lower Greenstones (Wilson, 1979), and include rocks of the 2.90-2.88 Ga Belingwean Group and rocks of the 2.83-2.79 Ga Lower Bulawayan Group (Horstwood et al., 1999; Wilson et al., 1995; Prendergast and Wingate, 2013). TTG-type granitoids of the Chingezi Suite (Wilson et al., 1995) are associated with the Lower Greenstones, and occur as intrusions within the Tokwe Segment to the west. These intrusions range in age from 2.98 Ga to 2.75 Ga (Nägler et al., 1997; Taylor et al., 1991; Horstwood 1999). They have been interpreted as the plutonic equivalents of the Belingwean and Lower Bulawayan felsic volcanic rocks (Luais and Hawkesworth, 1994).

Tectono-magmatic events that occurred in the Zimbabwe Craton at 2.75-2.62 Ga produced greenstone successions referred to as the Upper Greenstones, and divided into two distinct successions (e.g. Jelsma and Dirks, 2002; Wilson, 1979), namely the Western Succession of Wilson (1979) or type 2 greenstones of Jelsma and Dirks (2002), indicative of arc magmatism and juvenile crust, and the Eastern Succession (Wilson, 1979) or Type 1 greenstones (Jelsma and Dirks, 2002), reminiscent of rift or back-arc environments.

The Shamvaian Group is a siliciclastic sedimentary succession and represents the uppermost and youngest unit of the greenstone belt stratigraphy (Fig. 1). The time of deposition is unknown, but age determinations of adjacent rocks in various greenstone belts bracket sedimentation to between 2.68 and 2.64 Ga (Jelsma et al., 1996; Wilson et al., 1995). The Shamvaian Group is similar to modern foreland and

forearc successions and formed during compressional or transtensional tectonics associated with accretionary processes (Hofmann et al., 2002; Hofmann et al., 2004).

Final stabilization of the craton was achieved around 2.60 Ga ago with the emplacement of large volumes of crustally-derived Chilimanzi suite granites (e.g. Frei et al., 1999; Jelsma et al, 1996; Jelsma and Dirks, 2002), followed by intrusion of the layered igneous complex of the Great Dyke at 2.575 Ga (Oberthür et al., 2002).

3. Methods

Six meta-sedimentary samples were collected from the Buhwa, Shurugwi, and Midlands greenstone belts (GB) as well as the Njiri metasedimentary complex (Fig. 1). Samples belong to the Sebakwian, Belingwean and Lower Bulawayan groups (Table 1). Sample selection was based on previous discoveries of ancient detrital zircons from the southern portion of the craton in the vicinity of the Tokwe segment (Dodson et al., 1988). Samples were also collected from the vicinity of the Rhodesdale terrain (Fig. 1) that was identified to host Palaeoarchaean gneisses (Horstwood et al., 1999). From this area, quarzites from the Sebakwian Group were specifically targeted, as these have never been subjected to detrital zircon dating and were previously regarded to be >3.35 Ga old (Wilson, 1968). A description of the pertinent field and regional geology is given in the supplementary material (Supplementary Material: SM: “Sample Description”).

Following separation of heavy minerals using standard magnetic and heavy liquid procedures, approximately 100-150 zircon grains were picked, mounted in epoxy resin, polished to expose their interior and imaged using cathodoluminescence (CL). Analysis by SIMS proceeded in two modes: an initial $^{207}Pb/^{206}Pb$ age “reconnaissance” was conducted to establish the general geochronological make-up

and to ensure inclusion of the most ancient grains. These measurements were then supplemented by data from a subsequent "full scan" U-Th-Pb analysis in the same zircon domain. This second run focused on zircon grains with magmatic zoning patterns based on CL imaging. Specifically, grains were targeted showing least-complex internal morphologies and the presence of oscillatory zoning (Nemchin et al., 2006). The proportion of common ^{206}Pb in measured ^{206}Pb was estimated from ^{204}Pb assuming a present-day Stacey and Kramers (1975) model for terrestrial Pb-isotope composition.

Subsequently, O and Hf isotopic compositions were measured in-situ by SIMS and LA-MC-ICPMS, respectively, using near-concordant (>90%) grains. Analytical details follow Kemp et al. (2015), Nemchin et al. (2006) and Whitehouse and Kamber (2005). Further details are provided in the SM ("Analytical Methods"), including U-Th-Pb, O and Hf isotopic ratios of detrital zircons (SM: Tables 1, 3) and measured O and Hf values for reference zircons (SM: Tables 2A, B).

4. Results: U-Pb, O and Hf isotope data

BUC1: quartzite (Buhwa Formation, Buhwa greenstone belt)

Twenty-seven U-Pb, 17 O and 14 Lu-Hf isotope data were obtained from 27 detrital grains. 118 reconnaissance ^{207}Pb/^{206}Pb dates range from 1.8-3.7 Ga (Fig 2A). The oldest, but discordant, date is c. 3.697 Ga. Seventeen U-Pb analyses are near-concordant (>90%) ranging from 3.10 to 3.59 Ga. In a probability density plot (PDP), these near concordant U-Pb analyses display several main peaks of ^{207}Pb/^{206P}b ages at 3.6, 3.5, 3.4, 3.3 and 3.1 (only one data point) Ga. When considering near-concordant analyses, Th/U ratios are not correlated with age or U-Pb disturbance and range from 0.2 to 1.4 (SM: Table 1). Twelve O isotope data lie within the range defined by zircon

in equilibrium with mantle oxygen ($\delta^{18}O$ = 5.3±0.6 ‰: Valley et al., 1994), whereas three data points plot significantly below and one data point above the mantle range (Fig. 3A). Initial $^{176}Hf/^{177}Hf$ ratios with a range from 0.28046 to 0.28064 increase with decreasing age and plot on, or below, the chondritic uniform reservoir (CHUR) (Fig. 3B).

Z12-1: sandstone (Mafic Formation, Midlands greenstone belt)

Reconnaissance $^{207}Pb/^{206}Pb$ measurements (n = 106) reveal a range in apparent ages from 3.0 Ga to 3.9 Ga. Thirty-nine of these grains were used to obtain full U-Pb, with a further six analyzed for O and Lu-Hf isotope data. Only 6 dates are near concordant, yielding a peak at 3.57 Ga, with two minor peaks at 3.55 and 3.58 Ga (Fig. 2B). The majority of U-Pb dates are aligned along a horizontal vector in Tera-Wasserburg space, implying that Pb loss occurred recently and therefore that most $^{207}Pb/^{206}Pb$ dates approximate the crystallization age of the source(s) (see "Provenance"). Th/U ratios (0.1-1.7, near-concordant analyses) cluster around 0.5, displaying no correlation with age or concordance (SM: Table 1). $\delta^{18}O$ values define a narrow range (5.5-6.5 ‰), with most zircons showing equilibrium with the mantle (Fig. 3A). Initial $^{176}Hf/^{177}Hf$ ratios cluster between 0.28040 and 0.28050 along, or below, the CHUR evolution line (Fig. 3B).

Z12-2: quartzite cobble (Wanderer Formation, Shurugwi greenstone belt)

Reconnaissance $^{207}Pb/^{206}Pb$ measurements (n=95) give a wide range of dates from 2.88 to 3.64 Ga. Out of 22 $^{207}Pb/^{206}Pb$ dates only 6 dates are near-concordant translating into a peak in a DP plot at 3.32 Ga (Fig. 2C). A similar peak is observed when all full U-Pb analyses are combined, although several older populations are

present in the latter dataset ranging from 3.40 to 3.70 Ga. The majority of the $^{207}Pb/^{206}Pb$ data scatter around a horizontal line projecting away from the Concordia curve, suggesting a minor effect of Pb loss on $^{207}Pb/^{206}Pb$ data. A primary magmatic origin of the near-concordant zircon is suggested by Th/U ratios of 0.1-1.2 (SM: Table 1), which are non-correlated with age or concordance. All six near-concordant zircons have mantle-like $\delta^{18}O$ values, within errors (Fig. 3A). Despite the narrow range in ages, $^{176}Hf/^{177}Hf$ ratios are strongly variable (0.28043 – 0.28069), plotting along and above CHUR and showing no correlation with age (Fig. 3B).

Z04-15: conglomerate (Wanderer Formation, Shurugwi greenstone belt)

Twenty grains were used to obtain twenty U-Pb and three O and Lu-Hf isotope data (Fig. 2D). The small number of near concordant dates (n=3) with ages between 3.54 and 3.70 Ga contrasts with the wide range of reconnaissance $^{207}Pb/^{206}Pb$ dates of 1.27-3.66 Ga, the latter showing no pronounced clusters in the PDP. This finding, coupled with the observation that discordant dates are not aligned along a horizontal vector, is consistent with ancient severe U-Pb isotopic disturbance rendering most dates unreliable. All three $\delta^{18}O$ values are within the mantle-equilibrium range (Fig. 3A). $^{176}Hf/^{177}Hf$ ratios plot along and slightly below the CHUR evolution line (Fig. 3B; only near-concordant grains). Th/U ratios (near-concordant analyses) show no systematic relationship with age or concordance, but suggest a magmatic origin for all grains (SM: Table 1).

Z10-3: quartzite (Njiri metasedimentary complex)

Reconnaissance $^{207}Pb/^{206}Pb$ measurements (n = 104) yield a wide range in apparent ages from 2.20 to 3.81 Ga. Of the full scan analyses (n = 56), 30 grains yielded near-

concordant U-Pb ages translating into one pronounced peak at 3.79 and several minor peaks between 3.37 and 3.75 Ga (Fig. 2E). The remaining analyses are scattered away from the Concordia curve, and it is difficult to distinguish between ancient and recent Pb loss. Th/U ratios range from 0.2 to 0.9 and are uncorrelated with age and concordance (SM: Table 1, near-concordant analyses). Out of thirty O isotope analyses ten older grains have mantle-like $\delta^{18}O$ values. Values generally increase with younger age (Fig. 3A), reaching up to 10 ‰. $^{176}Hf/^{177}Hf$ ratios define a narrow range (0.28027 - 0.28037) that is less radiogenic than CHUR, with the exception of one grain (Fig. 3B).

Z10-4: quartzite (Njiri metasedimentary complex)

Only four of 38 U-Pb dates are near-concordant translating into four spikes in the PDP at 3.39 to 3.64 Ga (Fig. 2F). When all $^{207}Pb/^{206}Pb$ ratios are combined into PD distributions, the data are not concentrated in distinct populations but smeared out towards younger ages, indicative of multiple (non-zero) Pb loss. Th/U ratios are within the same range as observed for all previous samples (0.2 – 0.9), with no correlation with age or concordance (SM: Table 1; near concordant analyses). Five of seven $\delta^{18}O$ values are within the mantle equilibrium range (Fig. 3A), while two are lower, possibly indicating low temperature alteration in their source region. $^{176}Hf/^{177}Hf$ ratios plot along or below CHUR (3 data points plot exactly on the model curve), with values of 0.28036 - 0.28057 (Fig. 3B).

5. Discussion

5.1 Primary versus secondary isotopic variations

The reliability of isotopic compositions of very ancient detrital zircon requires critical assessment in view of several previous studies having highlighted potentially serious complications (e.g. Amelin et al., 1999; Gerdes and Zeh, 2009; Kemp et al., 2010; Nemchin et al., 2006; Zeh et al., 2014; Vervoort and Kemp, 2016). Herein, several criteria were employed to establish primary isotopic compositions: (i) $^{207}Pb/^{206}Pb$ analyses obtained from the same domain of a zircon grain from both runs (reconnaissance and full analysis) agree within analytical error (SM: "Cathodoluminescence Imaging and Description of Internal Zircon Structures": Fig. 1, Fig. 3, e.g. grain Z10-3/18). (ii) Analyses of zircon with Th/U<0.1 were rejected (Hoskin and Schaltegger, 2003) as they may reflect metamorphic growth. (iii) A number of zircon grains were also subjected to multiple spot analyses for O and Hf within the same zircon domain. Coupled Hf and O data were found to be identical within analytical uncertainty, (SM: "Cathodoluminescence Imaging and Description of Internal Zircon Structures": Fig. 2A, B) for zircon domains with identical age, testifying to reliable isotopic memory. Finally, for zircon from all studied samples, interpretation of O and Hf isotope systematics is limited to analyses with discordance <10%.

One important requirement for reliable estimation of initial ε_{Hf} is that the Hf isotope data are associated with an accurate crystallization age. For instance, using detrital zircon from the Limpopo Belt, Zeh et al. (2008) observed constant $^{176}Hf/^{177}Hf$ and concomitant decrease in ε_{Hf} for zircon younger than ~3.3 Ga. This observation was explained in terms of ancient Pb loss, resulting in artificially lower calculated ε_{Hf} values. In contrast, the Zimbabwean detrital zircon dataset overall shows initial Hf isotopic ratios that increase with decreasing age, accompanied by decreasing ε_{Hf} values when individual samples are considered, except for sample Z12-2 (Fig 3B, C).

In the Tera-Wasserburg diagram, many zircon grains plot on a horizontal vector, suggestive of recent Pb loss, while scatter hints at multiple Pb loss events. In conventional Concordia diagrams, discordant Archaean zircons often exhibit trends towards non-zero lower intercepts attributed to the dissimilar chemical behaviour of ^{207}Pb and ^{206}Pb in damaged crystal lattice (Kramers et al., 2009).

Sample Z10-3 shows a smear along conventional Concordia (not shown) and what could be interpreted as a sub-horizontal, albeit scattered, $^{176}Hf/^{177}Hf$ – time array (but see below) that could signal ancient Pb loss (Fig. 3B). Zircons from this sample also display a wide range in $\delta^{18}O$ values from +5.0 to +9.6 ‰, potentially implying variable exchange between radiation-damaged zircon and fluids (e.g. Hoskin and Schaltegger, 2003). This sample is therefore particularly well suited for assessing post-magmatic alteration. Examination of CL images of selected grains of this sample identified two groups (reported in SM: "Cathodoluminescence Imaging and Description of Internal Zircon Structures": Fig. 3): group (1) zircons with O isotopic compositions within 5.3±0.6 ‰ (Fig. 4A), and group (2) zircons with non-mantle-like O isotopic values but showing primary magmatic, undisturbed microstructural features (Fig. 4B). Group (1) zircons display microstructures that indicate some modification of primary igneous features, including faded zoning, discontinuous curved zoning and irregular replacement by homogeneous, CL-brighter material. Despite textural evidence for some recrystallization, analyzed zircon domains appear to have preserved (primary) magmatic O isotopic compositions (4.7 ‰ < $\delta^{18}O$ < 5.9 ‰). On the other hand, group (2) zircons show no or little evidence for textural overprinting, except for some grains having thin rims of newly formed zircon, but yield $\delta^{18}O$ > 6 ‰. In all examined cases, however, Th/U values are consistent with magmatic growth. It is concluded that $\delta^{18}O$ values > 6 ‰ and U-Pb ages <3.8 Ga do

not represent significant post-magmatic disturbance and open-system behavior. Evidence for preserved primary isotopic zircon compositions is also provided by two identical (within errors) $^{207}Pb/^{206}Pb$ ages, and identical (within errors; Pb ages and $\delta^{18}O$: 1σ, ε_{Hf}: 2σ) O and Hf isotopic compositions and Th/U values obtained by multiple SIMS analyses within one grain belonging to group (1) (Fig. 4A).

Since radiation-damaged zircon is particularly prone to exchange with fluids and loss of Pb (e.g. Geisler et al., 2002), we also examined the relationship between O isotope systematics, discordance and the degree of metamictization for grains of sample Z10-3. Partial Pb-loss would have occurred most probably during the 3.35 Ga event, which marks widespread crustal reworking (see below), while disturbance of primary O isotopic compositions may have taken place at any time. Assuming that the total accumulative dose Dα (α-decay events/mg: Ewing et al., 2000) is a meaningful proxy for the degree of metamictization (details are provided in the SM: "Estimation of radiation dose as proxy to metamictization in zircon"), based on the concept of "percolation point" (Salje et al., 1999), it can be concluded that most of the zircons belonging to Z10-3 did not experience extensive degrees of metamictization, and therefore behaved in a closed-system fashion with respect to O, U-Pb and Hf. The sub-horizontal Hf-age array (Fig. 3B) does not arise from simple Pb loss from a single-age source component considering the scatter, but likely reflects a composite reworking trend (i.e. source heterogeneity). Furthermore, Pb loss would manifest itself in a near-horizontal trend, which is not exactly observed for the current dataset, specifically for analyses of sample Z10-3. The geological process and environment responsible for the correlated U-Pb, O and Hf isotopic arrays in >3.6 Ga zircons is further discussed below.

5.2 Provenance

Age spectra of detrital zircons derived from several locations within the central and most ancient part of the Zimbabwe Craton are compared in Fig. 5. The age of sedimentation remains poorly constrained, but existing data (e.g. Dodson, et al., 1988) and new ages reported here indicate deposition after 3.1 Ga, including the Sebakwian Group sedimentary rocks. We thus infer Zimbabwe Craton evolution during Palaeoarchaean and earlier times, i.e., during the early stages of craton growth, from detrital, originally igneous zircon. Importantly, local provenance is indicated for several reasons (see also SM: "Sample Description"): (i) Immaturity of sediments from the Shurugwi greenstone belt reflects low degrees of reworking and thus transport. (ii) Detrital ages of quartzite from the Mafic Formation sitting immediately above granitic basement and containing abundant zircons with the age identical to underlying basement (see below). (iii) While no detailed sedimentological information is available for the Sebakwian Group, Zr concentrations of the dated samples are <70 ppm (SM: Table 4), thus suggesting minimal to moderate reworking of the detritus. (iv) Isotope (Nd and Pb) and REE+Y characteristics of chemical sediments in the 2.7 Ga greenstone belts (Bolhar et al., 2002) and 2.9 Ga greenstone belts (Kamber et al., 2004), showing that the dissolved load was locally sourced.

The distribution of near-concordant $^{207}Pb/^{206}Pb$ ages appears episodic for individual locations and for all data combined ("Zimbabwe Craton", Fig. 5), although the total number of analyses (N=165) for the craton is modest compared to datasets for other similarly-aged cratons (e.g. Beartooth Mountain quartzites: Wyoming Craton; Mueller and Wooden, 2012). If the age distribution is not an artifact of the relatively small volume of data, it could indicate localized provenance (see above), preservational bias (see below) or true pulses in magmatic activity. The most

prominent, and also oldest peak, at 3.79 Ga is largely derived from metaquartzite Z10-3 from the Njiri metasedimentary complex, with some contribution from the Buhwa GB. A 3.8 Ga age population has been previously recognized there by Dodson et al. (1988), who speculated that these grains were derived from a proximal basement source due to their relatively high abundance in the studied sample. The second most ancient peak at 3.70 Ga is observed for detritus from the Shurugwi GB (data from Nägler et al. 1997, their Table 1). No exposed crust with an age of >3.6 Ga is currently documented from Zimbabwe. Minor peaks in probability density plots occur at 3.6 Ga in zircon from the Njiri Complex and the Wanderer Formation. No magmatic event is known for this time, although Wilson et al. (1995) reported one inherited grain extracted from a 2.66 Ga banded felsite of the Upper Shamvaian Group dated at 3.62 Ga. The same sample also yielded a xenocrystic grain dated at 3.55 Ga, an age which is reflected in abundance peaks at 3.53 to 3.57 Ga for most locations. The 3.5-3.6 Ga detrital signal coincides with emplacement of the Sebakwe River Gneiss, exposed in the Midlands GB north of the Towke segment and dated at 3.565±21 Ga (U-Pb zircon: Horstwood et al., 1999). The nonconformable relationship between sandstone Z12-1 (Mafic Formation) and the Sebakwe River Gneiss is reflected clearly in the prominent abundance peak at ~3.57 Ga (Fig. 2). A Discordia line using all detrital data translates into an upper intercept age of c. 3.57 Ga (not shown). Hence, detrital zircon from the Mafic Formation was largely derived from erosion of the Sebakwe River Gneiss, currently considered the oldest dated magmatic rock in the Zimbabwe Craton. A c. 3.45 Ga event is recorded in detrital ages from the Shurugwi, Buhwa and Belingwe GBs (Fig. 5). This event overlaps with emplacement of the 3.456±6 Ga Kwekwe Gneiss, representing the western margin of the Rhodesdale granitoid-gneiss complex, and the 3.455±2 Ga Tokwe River Gneiss, part

of the Tokwe segment. The similarity in crystallization ages between both gneiss units prompted Horstwood et al. (1999) to infer a substantially larger spatial extent of the Tokwe segment than was previously assumed. They noted that the c. 3.45 Ga magmatic event is also strongly represented in early Rb-Sr and Pb-Pb whole rock isotope studies (Taylor et al., 1991). Using existing geochronological data and field relationships, these authors interpreted 3.35 Ga ages to reflect a widespread crustal melting event, possibly resulting in crustal stabilization of the Tokwe segment. The Mont d'Or granitoid in the north-western Tokwe segment (Fig. 1) yielded a whole rock Pb-Pb regression date of 3.35 Ga and its very elevated $^{207}Pb/^{204}Pb$ initial ratio necessitates anatectic reworking of much older crust (Taylor et al., 1991). Its emplacement was coeval with migmatitic reworking of the Tokwe River Gneiss, as constrained by a 3.368±9 Ga U-Pb zircon age of leucosome (Horstwood et al., 1999). Crystallization of the Mushandike granite occurred at around 3.37 Ga (Dodson et al., 2001). A prominent role for this magmatic event is clearly reflected in our compilation of detrital ages showing contemporaneous c. 3.37 Ga peaks in the Njiri complex, Shurugwi GB and the Manjeri Formation of the Belingwe GB (Fig. 5). Evidence is documented in detrital age peaks for a 3.2 Ga event. The nature of this event remains poorly understood, and only one 3.2 Ga zircon age has been reported from a granitic pebble in Shamvaian conglomerate (Dougherty-Page, 1994). The geological significance of this cryptic age cannot be further substantiated. One concordant zircon date of 3.1 Ga was found for the Buhwa Formation quartzite (Fig. 2). Two dates of 3.1 Ga were also previously reported for a Buhwa quartzite (Dodson et al., 1988). This grain yields a mantle-like O isotopic composition, and may reflect crystallization of the Shabani Gneiss for which Taylor et al. (1991) reported a Pb-Pb whole rock date of 3.088±45 Ga. Finally, we note that the close correspondence in

ages derived from detrital (this study) and magmatic (published) zircon strongly suggests that the record retrieved from Sebakwian, Belingwean and Bulawayan metasedimentary rocks is a reliable proxy to the crustal evolution of the Zimbabwe Craton until ~3.1 Ga.

5.3 Melt extraction, crust formation and reworking

Approximately half of all zircons have $\delta^{18}O$ values consistent with crystallization in equilibrium with mantle-derived melts (5.3±0.6 ‰, 2σ: Valley et al., 1994). The remaining zircon with higher $\delta^{18}O$ values (mostly from Z10-3) crystallised from melts that had incorporated variable amounts of material previously subjected to hydrothermal/surface alteration, thus reflecting magmatic reworking. Significantly, 3.6–3.8 Ga zircon data belonging to the Njiri complex reveal distinctive correlations of Hf and O isotopic compositions with age (Fig. 3A, C), and also display the most elevated $\delta^{18}O$ values. In contrast, <3.6 Ga zircon O isotope values largely overlap the mantle range, with five data points plotting at lower values.

The majority of the post 3.6 Ga Hf data (with the exception of four analyses) straddle CHUR, within analytical errors. Resolvable, supra-chondritic data points only appear at 3.35 Ga. The absence of supra-chondritic Hf values argues against a strongly depleted early Archaean mantle underlying the craton that was tapped by younger magmas, in agreement with the zircon Hf isotopic record worldwide (Vervoort et al., 2012, 2015). Chondritic and sub-chondritic, age-corrected $^{176}Hf/^{177}Hf$ (Fig. 3B) define one distinct, and three less well-defined, ε_{Hf}-time arrays (Fig. 3C).

These arrays in initial ε_{Hf} - zircon crystallization age space allow estimation of the average $^{176}Lu/^{177}Hf$ of the source of melts from which zircon crystallized (Amelin et al., 1999). Regression of data points with mantle $\delta^{18}O$ values (weighted by

analytical error using Isoplot: Ludwig, 2001; details are given in the caption to Fig. 3) yields $^{176}Lu/^{177}Hf$ of 0.011±3 to 0.022±23 (2σ). Data from zircon with mantle and non-mantle like $\delta^{18}O$ values overlap or plot along identical trajectories (Fig. 3A, C). Low MSWDs (<1.5) signify extraction from relatively homogenous sources. Representative mean ratios of $^{176}Lu/^{177}Hf$ for mafic lithologies range from 0.026 (MORB), 0.029 (oceanic plateau basalt), 0.033 (chondrite) and 0.03-0.009 (oceanic and continental arc lavas), in contrast to values of 0.012-0.015 (continental crust) and <0.01 (TTGs) (Goodge and Vervoort, 2006; Blichert-Toft and Albarede, 2008; Chauvel et al., 2014). There was apparently little scatter in source $^{176}Lu/^{177}Hf$ probably reflecting high-degree melting of ordinary mantle. Source $^{176}Lu/^{177}Hf$ >0.01 estimated from Zimbabwean detrital zircons renders TTG-like material as source reservoir unlikely, and favours mafic to intermediate crustal source compositions. It is noted that estimated source $^{176}Lu/^{177}Hf$ is dependent on the inclusion/exclusion of data with extreme values (e.g. ε_{Hf} values of -5 and -8 for sample Z10-3; Fig. 3C). However, to minimise bias only those data points were excluded from regression that clearly plotted off any particular array. Thus, almost all data were included in regressions. Absence of distinctly suprachondritic ε_{Hf} values in early Archaean zircon has also been reported, for instance, from the Narryer Gneiss Complex, Yilgarn Craton (Kemp et al., 2010), Pilbara Craton (Kemp et al., 2015) and the Beartooth Mountain quartzites, Wyoming Craton (Mueller and Wooden, 2012; Figure 3D~~).~~

5.4 Global crust formation events or preservational bias?

When all detrital zircon data are combined in a PDP (Fig. 5), the Palaeo-Eoarchaean crustal evolution of the Zimbabwe Craton appears to be punctuated by abundance peaks in crystallization ages at 3.8-3.7, 3.6 and 3.4-3.3 Ga. Episodic crustal growth or

preservation is also manifested in linear arrays in ε_{Hf}-time space. Punctuated crust-forming episodes have been known from both U-Pb zircon crystallization ages (e.g. Condie, 1998) and Nd-Sr isotopes of mantle derived rocks (e.g. Stein and Hofmann, 1994). Crustal age peaks may, however, also reflect periods during which preservation of the rock record was enhanced in particular geodynamic settings (Hawkesworth et al., 2009).

The question arises whether peaks in U-Pb and Hf model ages apparent in the Zimbabwean dataset can be correlated with information from other cratons during 4.0 to 3.0 Ga, especially those that share a similar geological record and carry the high-μ isotopic signature (North Atlantic, Slave, Zimbabwe, Yilgarn, and Wyoming). Using baddeleyite U-Pb ages of mafic dyke swarms Söderlund et al. (2010) inferred that the Zimbabwe and Kaapvaal cratons did not amalgamate into a coherent block (Kalahari) until ~2.0 Ga, well outside the time window considered in this study. Several other major differences in geology also suggest that both cratons do not have a shared history prior to 2.0 Ga, such as missing equivalents of the ~2.0 Ga Bushveld Complex in Zimbabwe and the 2.6 Ga Great Dyke in South Africa (Bleeker, 2003). Instead, palaeomagnetic and geochronogical information is consistent with reconstruction of a supercontinent in the Neoarchaean, comprising the Zimbabwe, Yilgarn, Slave and various other cratons (Bleeker, 2003; Söderlund et al., 2010; Prendergast and Wingate, 2013). Zircons from the ~3.73 to 2.65 Ga Narryer Gneiss Complex (NGC) in the Yilgarn Craton (Kinny et al., 1988; Kemp et al., 2010) document major crust formation and reworking events during similar times as seen on the Zimbabwe Craton. In ε_{Hf} – time space (Fig. 3D)., both datasets point to extraction events from chondritic or slightly depleted mantle at 3.85-3.9 Ga and 3.7 and record crustal reworking at 3.3 Ga. Zircon age clusters at 3.4, 3.6 and 3.8 Ga for detrital zircon of

the Jack Hills metasedimentary belt, contained within the NGC were also reported by Bell et al (2011). Detrital zircons from the Slave Craton register several magmatic episodes with melts extracted from the mantle at 3.4 - 3.3 Ga and 3.8 - 3.7 Ga, likewise similar to what is observed here for the Zimbabwe Craton. Detrital zircon $\delta^{18}O$ values from the Slave Craton show a shift from mostly mantle-like after 3.2 Ga to values >6 ‰, whereas most O isotope values for Zimbabwe are mantle-like (Fig 3E). Major magmatic episodes in the Slave Craton were inferred to reflect global rather than regional events (Pietranik et al., 2008), and the coincidence with Zimbabwean age clusters is consistent with a global growth/reworking pattern. Geological similarities were recognized between the Slave, Wyoming and Zimbabwe cratons (Bleeker, 2003). A broad array in the Wyoming data extending from chondritic ε_{Hf} values at 4 Ga towards values of -10 over a period of almost 600 m.y. extends subparallel, but along more unradiogenic values, to the 3.8–3.6 Ga array seen in the Zimbawean record (Fig. 3D). The data cluster for the Wyoming Craton at 3.4 - 3.5 Ga is unmatched in the Zimbabwean dataset. Up to five distinct, major tectono-thermal events are preserved in the oldest known crustal rocks on Earth, the Acasta Gneiss Complex (AGC) in the Slave Craton, namely at ~4.0 Ga, ~3.9 Ga, ~3.7 Ga, ~3.6 Ga and ~3.35 Ga (Stern and Bleeker, 1998; Bowring and Williams, 1999; Iizuka et al., 2007; Mojzsis et al., 2014; Reimink et al., 2016). These age groups reflect protolith emplacement, high-grade metamorphism (including migmatization), deformation and later-stage intrusive events. Despite the geological complexity and antiquity, and the geochronological and petrological heterogeneity, the broad similarity in age peaks (besides at ~4 Ga) between Acasta Gneiss and detrital zircons from the Zimbabwe Craton is nevertheless striking, and further hints at an apparent global pattern of tectono-thermal pulses documented across several Archaean crustal

domains, including Zimbabwe. A scattered band defined by 4.0 to 3.6 Ga old zircons from the Acasta Gneiss Complex (felsic orthogneisses: Bauer et al., 2017) in ε_{Hf} vs time age space (Fig 3D) runs sub-parallel, but along more unradiogenic Hf values, when compared to the >3.6 Ga Zimbabwean trend. While the Acasta data point towards older (up to 4.2 Ga), long-lived lithosphere, trends in both datasets (and also in the Narryer Gneiss Complex) are consistent with a lack of input from depleted/chondritic mantle sources over an extended period of time. Reworking affected both regions at 3.5 Ga and 3.3 Ga, possibly indicative of a coeval tectono-thermal event in both cratons. Representative Eoarchaean TTGs from the Itsaq Gneiss Complex (IGC) formed during a period of 180 m.y. (3.9-3.7 Ga), and their initial Hf isotopic ratios are CHUR-like within errors (Hiess et al., 2009; Kemp et al., 2009; Næraa et al. 2012). Initial Hf values for zircons from IGC gneisses partly overlap and extend the data array displayed by 3.8-3.6 Ga Zimbabwean detrital zircons (Fig. 3D).

In summary, the apparent "global" coincidence of age peaks and Hf isotope-time patterns supports the notion that crustal blocks with preserved >3.8 Ga zircon that are presently separated over long distances once formed a cratonic entity (possibly the "high-μ craton": Kamber, 2015), that has since rifted apart and subsequently been dispersed around the planet.

5.5 Significance of zircon oxygen isotope data

The similar and overlapping zircon ε_{Hf}-time patterns for the Itsaq Gneiss Complex and the Zimbabwe detrital zircon dataset do not extend to zircon $\delta^{18}O$ values, which are largely mantle-like (mean compositions of 4.9 - 5.1 ‰) in the case of the IGC. Hiess et al. (2009) interpreted Hf and O isotope systematics for Eoarchaean TTG in the IGC in terms of melting of hydrated mafic source material, either in a subduction

zone environment or at the base of an overthickened oceanic plateau. Generally elevated $\delta^{18}O$ values for the Zimbabwean detrital zircon dataset may therefore reflect a larger proportion of hydrated or hydrothermally altered mafic crust involved in melting to form TTG-like protoliths. This is suggested in particular by zircons from sample Z10-3, where zircon $\delta^{18}O$ increases from mantle-like to ~ 10‰ with decreasing age along what appears to be a closed system reworking trend in Hf isotope-time space. The petrogenetic significance of this distinctive trend is difficult to reconstruct from detrital zircons, but the pattern is consistent with the progressive burial (possibly through volcanic resurfacing or imbrication) and dehydration of altered mafic to intermediate source rocks. The accumulating effects of rock-fluid interaction at various crustal levels would have imprinted increasingly heavier O isotopic signatures on partial melts with time, potentially explaining the co-evolution of O and Hf from 3.8 to 3.6 Ga. This highlights the critical role of fluid release, perhaps accompanied by internal radioactive heat production, for protracted crustal melting over >200 m.y. Survival of portions of Eoarchaean lithosphere (on the high-μ craton) was possible for several hundred million years due to the presence of an underlying, sufficiently deep and refractory lithospheric mantle root (e.g. Kamber, 2015).

Final remarks

Detrital zircons exhibit O-Hf isotope systematics consistent with predominantly juvenile crust formation through the earliest history of the Zimbabwe Craton from 3.8 until 3.35 Ga. At around 3.35 Ga, broadly coinciding with stabilization of the oldest segment of the craton (Tokwe), a switch in geodynamic regime may have caused major reworking of ancient crust including high-grade metamorphism. Prior to 3.35

Ga, suprachondritic Hf isotope signatures in zircon are essentially absent, suggesting that melts derived from a mantle that had seen little depletion. There is a growing body of geochemical and geochronological data, suggesting that the Tokwe segment, originally proposed by Wilson (1990) to encompass (just) a group of ~3.5 Ga gneisses and supracrustal rocks north and east of Zvishavane, may be of substantial lateral extent. Kusky (1998) and Horstwood et al. (1999) inferred that >3.0 Ga old basement may be distributed over an area with an extension of greater than 450 km. Major (and multiple?) melt depletion events and concomitant stabilization of lithospheric mantle would have likely affected large portions of the craton, a notion strongly supported by Os isotope systematics derived from the southern (Smith et al., 2009) and central (Nägler et al., 1997) lithospheric mantle. Ancient crust is also preserved as 2.6 – 2.7 Ga TTG-type granulites in the North Marginal Zone of the Limpopo Belt bordering the southern edge of the Zimbabwe craton, which were formed by remelting of an old (>3.25 Ga), high-μ source (Berger and Rollinson, 1997). A distinct group of zircons (up to 3.8 Ga) appears to be derived from an altered mafic crustal source extracted from chondritic mantle at ca. 3.85-3.9 Ga that evolved in isolation for a period of 200 m.y., during which reworking produced melts with progressively more negative ε_{Hf} and elevated $\delta^{18}O$ signatures.

Acknowledgements

RB acknowledges support through grants from the University of Queensland and the Australian Research Council; the latter also supported TK through a Future Fellowship (FT100100059). AH acknowledges financial support by the National Research Foundation of South Africa, and provision of office space and logistical support from the Department of Geology, University of Zimbabwe. SW was

supported by a DAAD Rise scholarship. Four anonymous reviewers provided detailed and constructive criticism. Roland Maas and Jan Kramers provided useful comments on an earlier version of the manuscript. Jane Blichert-Toft and Marc Norman are thanked for their editorial input.

Figure Captions

Figure 1

Simplified geological map of the central portion of the Zimbabwe Craton, showing sample locations (adopted from Wilson, 1990).

Figure 2

U-Pb Tera-Wasserburg diagrams for detrital zircons from the Zimbabwe Craton. Error bars represent errors quoted in SM Table 1 of SM, and are generally smaller than symbols. Inset diagrams show probability density plots using data obtained by reconnaissance and full scan analysis (see methods); full scan data with concordance >90% ("concordant") are distinguished from all data; "N" refers to the number of discordant and concordant data from the full scan analysis; (A) Buhwa Greenstone Belt (GB); (B): Shurugwi GB; (C) Midlands GB; (D) Midlands GB; (E, F) Njiri metasedimentary complex. GB = Greenstone Belt.

Figure 3

O and Hf isotopic data for detrital zircon from the Zimbabwe Craton vs. $^{207}Pb/^{206}Pb$ ages; $\delta^{18}O=([^{18}O/^{16}O sample]/[^{18}O/^{16}O standard_{V\text{-}SMOW}]\text{-}1)x1000$ ‰), $\varepsilon_{Hf}= [^{176}Hf/^{177}Hf$ sample]/[$^{176}Hf/^{177}Hf$ chondritic reservoir]-1x10000). At the inferred crystallisation

age, initial $\varepsilon_{Hf}(t)$ values were calculated using the CHUR (chondritic uniform reservoir) parameters of Bouvier et al. (2008) viz., $^{176}Hf/^{177}Hf_{CHUR}$ = 0.282785 and $^{176}Lu/^{177}Hf_{CHUR}$ = 0.0336 and the decay constant of $\lambda^{176}Lu$ = 1.867 x $10^{-11}yr^{-1}$ (Scherer et al., 2001; Söderlund et al., 2004). Hf isotopic evolution of the Depleted Mantle (DM) was determined using $^{176}Hf/^{177}Hf_{DM}$ = 0.283238 and $^{176}Lu/^{177}Hf_{DM}$ = 0.03976 (Vervoort et al., 2015). (A) O isotopic compositions (error bars = 1σ) for the majority of zircons with ages <3.6 Ga plot within the range defined by zircon that crystallized in magmatic rocks with a mantle-like oxygen isotope composition ($\delta^{18}O$=5.30±0.6, 2σ: Valley et al., 1994), consistent with derivation from mantle-derived melts; zircons with ages >3.6 Ga define a trend of increasing $\delta^{18}O$ with decreasing age, consistent with progressive low-temperature alteration in surface environments as a function of time. (B) Approximately half of all initial $^{176}Hf/^{177}Hf$ data (error bars = 2σ) straddle the chondritic reference line, suggesting derivation from undifferentiated mantle sources. A regression line (stippled) based on all data from sample Z10-03, excluding two analyses with ages <3.4 Ga, contrasts with a horizontal Pb loss trend shown for comparison. (C) Zircon data define several linear arrays in ε_{Hf} vs time space, indicative of episodic crust formation from chondritic mantle sources. Regression lines (weighted according to analytical error) were based on zircon data with mantle-like O isotopic compositions and yield $^{177}Lu/^{176}Hf$ ratios of source materials. Almost all data points were assigned to any of the trends (number of data points used in regression is indicated by "n", data grouped together are encircled: Fig. 3C). Regression of data using only mantle-like $\delta^{18}O$ and combined data (mantle and non mantle-like) yielded indistinguishable slopes. DM = Depleted Mantle, CHUR = chondritic uniform reservoir. Small symbols (B, C): 4.7‰≤$\delta^{18}O$≥5.9‰, large symbols: 4.7‰>$\delta^{18}O$<5.9‰. (D) Compilation of single

zircon $\varepsilon_{Hf}(t)$ vs $^{207}Pb/^{206}Pb$ ages from 4 to 3 Ga for cratons with a high U/Pb (high-μ) source signature; (E) compilation of $\delta^{18}O$ vs age for a subset of the same data. Data sources: Acasta Gneiss Complex (TTGs: Bauer et al., 2017); Itsaq Gneiss Complex (TTGs: Hiess et al., 2009; Kemp et al., 2009); Slave Craton (detrital: Pietranik et al., 2008); Wyoming Craton (detrital: Mueller and Wooden, 2012); Narryer Gneiss Complex (gneisses, granites: Kemp et al., 2010), Pilbara Craton (tonalite: Kemp et al., 2015). Also shown are detrital zircon data from the Limpopo Belt (Zeh et al., 2014). The bulk of the latter data does not reveal any distinct evolutionary trends, but instead shows overlap with data from all other cratonic regions, including the Zimbabwe Craton.

Figure 4

Cathodoluminescence images of zircon grains representative of groups (1) and (2). A (Group 1): disturbed/complex microstructures, mantle-like $\delta^{18}O$: subhedral, short-prismatic zircon with complex zoning and thin rims. Two SIMS analyses targeting the interior of the grain yielded semi-identical Th/U, $\delta^{18}O$, εHf and U-Pb ages (. B (Group 2): magmatic microstructures, non-mantle-like $\delta^{18}O$): subhdral, short-prismatic zircon showing oscillatory zoning, an inherited core and one to two rims. One SIMS analysis targeting the outer magmatic core of the grain yields a non-magmatic $\delta^{18}O$ value.

Figure 5

Probability Density (DP) plots based on detrital zircon data (concordance>90%, except Basal Succession of Shurugwi GB and Brookland Formation of Belingwe GB: no concordance information available) from individual locations within the

Zimbabwe Craton; from left to right: Njiri metasedimentary complex (this study), Shurugwi GB (Basal Succession: Nägler et al. 1997), Shurugwi GB (Wanderer Formation: this study, Dodson et al., 1988), Buhwa GB (this study, Dodson et al., 1988), Belingwe GB (Brooklands Formation: Hunter, 1997), Belingwe GB (Manjeri Formation) and all data combined (Zimbabwe Craton).

References

Amelin, Y., Lee, D.C., Halliday, A.N. and Pidgeon, R.T. (1999) Nature of the Earth's earliest crust from hafnium isotopes in single detrital zircons. *Nature* **399**, 252-255.

Bauer, A.M., Fisher, C.M., Vervoort, J.D. and Bowring, S.A. (2017) Coupled zircon Lu–Hf and U–Pb isotopic analyses of the oldest terrestrial crust, the> 4.03 Ga Acasta Gneiss Complex. *Earth and Planetary Science Letters* **458**, 37-48.

Berger, M. and Rollinson, H. (1997) Isotopic and geochemical evidence for crust-mantle interaction during late Archaean crustal growth. *Geochimica et Cosmochimica Acta* **61**, 4809-4829.

Bell, E.A., Harrison, T.M., McCulloch, M.T. and Young, E.D. (2011). Early Archean crustal evolution of the Jack Hills Zircon source terrane inferred from Lu–Hf, $^{207}Pb/^{206}Pb$, and $\delta\ ^{18}O$ systematics of Jack Hills zircons. *Geochimica et Cosmochimica Acta* **75**, 4816-4829.

Berger, M. and Rollinson, H. (1997) Isotopic and geochemical evidence for crust-mantle interaction during late Archaean crustal growth. Geochimica et Cosmochimica Acta 61, 4809-4829.

Bleeker, W. (2003). The late Archean record: a puzzle in ca. 35 pieces. *Lithos* **71**, 99-134.

Blichert-Toft, J. and Albarede, F. (2008) Hafnium isotopes in Jack Hills zircons and the formation of the Hadean crust. *Earth and Planetary Science Letters* **265**, 686-702.

Bolhar, R., Hofmann, A., Woodhead, J. D., Hergt, J.M., and Dirks, P.H.G.M. (2002) Pb- and Nd-isotope systematics of stromatolitic limestones from the 2.7 Ga Ngezi Group of the Belingwe Greenstone Belt: constraints on timing of deposition and provenance. *Precambrian Research*, **114,** 277-294.

Bouvier, A., Vervoort, J.D. and Patchett, P.J. (2008) The Lu-Hf and Sm-Nd isotopic composition of CHUR: Constraints from unequilibrated chondrites and implications for the bulk composition of terrestrial planets. *Earth and Planetary Science Letters* **273**, 48-57.

Bowring, S.A. and Williams, I.S. (1999) Priscoan (4.00–4.03 Ga) orthogneisses from northwestern Canada. *Contributions to Mineralogy and Petrology* **134**, 3-16.

Cavosie, A.J., Valley, J.W. and Wilde, S.A. (2005) Magmatic $\delta^{18}O$ in 4400–3900 Ma detrital zircons: a record of the alteration and recycling of crust in the Early Archean. *Earth and Planetary Science Letters*, ***235***(3), 663-681.

Chauvel, C., Garçon, M., Bureau, S., Besnault, A., Jahn, B. M. and Ding, Z. (2014) Constraints from loess on the Hf–Nd isotopic composition of the upper continental crust. *Earth and Planetary Science Letters*, ***388***, 48-58.

Condie, K.C., (1998) Episodic continental growth and supercontinents: a mantle avalanche connection? *Earth and Planetary Science Letters* **163**, 97-108.

Dodson, M.H., Compston, W., Williams, I.S., & Wilson, J.F. (1988) A search for ancient detrital zircons in Zimbabwean sediments. *Journal of the Geological Society*, ***145***(6), 977-983.

Dodson, M.H., Williams, I.S. and Kramers, J.D. (2001) The Mushandike granite: further evidence for 3.4 Ga magmatism in the Zimbabwe craton. *Geological Magazine* **138**, 31-38.

Dougherty-Page, J.S., (1994) The evolution of the Archaean continental crust of northern Zimbabwe. Open University, Milton Keynes, UK.

Ewing, R. C., et al. (2000) Radiation-induced amorphization. *Reviews in mineralogy and geochemistry* **39**, 319-361.

Fedo, C.M., Eriksson, K.A. and Blenkinsop, T.G. (1995) Geologic history of the Archean Buhwa greenstone belt and surrounding granite-gneiss terrain, Zimbabwe, with implications for the evolution of the Limpopo Belt. *Canadian Journal of Earth Sciences* **32**, 1977-1990.

Frei, R., Schoenberg, R. and Blenkinsop, T.G. (1999) Geochronology of the late Archaean Razi and Chilimanzi suites of granites in Zimbabwe; implications for the late Archaean tectonics of the Limpopo Belt and Zimbabwe Craton. *South African Journal of Geology* **102**, 55-63.

Froude, D.O., Ireland, T.R., Kinny, P.D., Williams, I.S., Compston, W., Williams, I.T. and Myers, J. S. (1983) Ion microprobe identification of 4,100–4,200 Myr-old terrestrial zircons. *Nature **304***, 616-618.

Geisler, T., Pidgeon, R. T., Van Bronswijk, W. and Kurtz, R. (2002) Transport of uranium, thorium, and lead in metamict zircon under low-temperature hydrothermal conditions. *Chemical Geology* **191**, 141-154.

Gerdes, A. and Zeh, A., (2009) Zircon formation versus zircon alteration - New insights from combined U-Pb and Lu-Hf in-situ LA-ICP-MS analyses, and consequences for the interpretation of Archean zircon from the Central Zone of the Limpopo Belt. *Chemical Geology* **261**, 230-243.

Goodge, J. W. and Vervoort, J. D. (2006) Origin of Mesoproterozoic A-type granites in Laurentia: Hf isotope evidence. *Earth and Planetary Science Letters* ***243*****,** 711-731.

Guitreau, M., Blichert-Toft, J., Martin, H., Mojzsis, S. J. and Albarède, F. (2012) Hafnium isotope evidence from Archean granitic rocks for deep-mantle origin of continental crust. *Earth and Planetary Science Letters* ***337***, 211-223.

Hawkesworth, C., Cawood, P., Kemp, T., Storey, C. and Dhuime, B. (2009) GEOCHEMISTRY A Matter of Preservation. *Science* **323**, 49-50.

Hawkesworth, C.J., Moorbath, S., Onions, R.K. and Wilson, J.F., (1975) Age relationship between greenstone belts and granites in Rhodesian-Archaean Craton. *Earth and Planetary Science Letters* **25**, 251-262.

Hiess, J., Bennett, V.C., Nutman, A.P. and Williams, I.S. (2009) In situ U–Pb, O and Hf isotopic compositions of zircon and olivine from Eoarchaean rocks, West Greenland: New insights to making old crust. *Geochimica et Cosmochimica Acta* **73**, 4489-4516.

Hofmann, A., Dirks, P. and Jelsma, H.A. (2002) Late Archaean clastic sedimentary rocks (Shamvaian Group) of the Zimbabwe craton: first observations from the Bindura-Shamva greenstone belt. *Canadian Journal of Earth Sciences* **39,** 1689-1708.

Hofmann, A., Dirks, P.H.G.M. and Jelsma, H.A. (2004) Clastic sedimentation in a late Archaean accretionary terrain, Midlands greenstone belt, Zimbabwe. *Precambrian Research* **129**, 47-69.

Horstwood, M.S.A., Nesbitt, R.W., Noble, S.R. and Wilson, J.F. (1999) U-Pb zircon evidence for an extensive early Archean craton in Zimbabwe: A reassessment of the timing of craton formation, stabilization, and growth. *Geology* **27**, 707-710.

Hoskin, P.W.O. and Schaltegger, U. (2003) The composition of zircon and igneous and metamorphic petrogenesis. *Reviews in mineralogy and geochemistry*, **53**, 27-62.

Hunter, M.A. (1997) The tectonic setting of the Belingwe greenstone belt, Zimbabwe. University of Cambridge, UK.

Iizuka, T., Komiya, T., Ueno, Y., Katayama, I., Uehara, Y., Maruyama, S., Hirata, T., Johnson, S.P. and Dunkley, D.J. (2007) Geology and zircon geochronology of the Acasta Gneiss Complex, northwestern Canada: new constraints on its tectonothermal history. *Precambrian Research* **153,** 179-208.

Jelsma, H.A., Dirks, P.H.G.M. (2002) Neoarchaean tectonic evolution of the Zimbabwe Craton. In *The Early Earth: Physical, Chemical and Biological Development* (eds. C.M.R. Fowler, C.J. Ebinger and C.J. Hawkesworth) Geological Society of London Special Publications, pp. 183-211.

Jelsma, H.A., Vinyu, M.L., Valbracht, P.J., Davies, G.R., Wijbrans, J.R. and Verdurmen, E.A.T. (1996) Constraints on Archaean crustal evolution of the Zimbabwe craton: a U-Pb zircon, Sm-Nd and Pb-Pb whole-rock isotope study. *Contributions to Mineralogy and Petrology* **124**, 55-70.

Kamber, B.S. (2015) The evolving nature of terrestrial crust from the Hadean, through the Archaean, into the Proterozoic. *Precambrian Research* **258**, 48-82.

Kamber, B.S., Bolhar, R. and Webb, G.E. (2004) Geochemistry of late Archaean stromatolites from Zimbabwe: evidence for microbial life in restricted epicontinental seas. *Precambrian Research* **132**, 379-399.

Kamber, B.S., Collerson, K.D., Moorbath, S. and Whitehouse, M.J. (2003) Inheritance of early Archaean Pb-isotope variability from long-lived Hadean protocrust. *Contributions to Mineralogy and Petrology* **145**, 25-46.

Kemp, A.I.S., Foster, G.L., Scherstén, A., Whitehouse, M.J., Darling, J. and Storey, C. (2009) Concurrent Pb–Hf isotope analysis of zircon by laser ablation multi-collector ICP-MS, with implications for the crustal evolution of Greenland and the Himalayas. *Chemical Geology* **261**, 244-260.

Kemp, A.I.S., Wilde, S.A., Hawkesworth, C.J., Coath, C.D., Nemchin, A., Pidgeon, R.T., Vervoort, J.D. and DuFrane, S.A. (2010) Hadean crustal evolution revisited: New constraints from Pb-Hf isotope systematics of the Jack Hills zircons. *Earth and Planetary Science Letters* **296**, 45-56.

Kemp, A.I., Hickman, A.H., Kirkland, C.L., and Vervoort, J.D. (2015) Hf isotopes in detrital and inherited zircons of the Pilbara Craton provide no evidence for Hadean continents. *Precambrian Research*, **261**, 112-126.

Kenny, G.G., Whitehouse, M.J. and Kamber, B.S. (2016) Differentiated impact melt sheets may be a potential source of Hadean detrital zircon. *Geology* **44**, 435-438.

Kinny, P.D., Williams, I.S., Froude, D.O., Ireland, T.R. and Compston, W. (1988) Early Archaean zircon ages from orthogneisses and anorthosites at Mount Narryer, Western Australia. *Precambrian Research* **38**, 325–341.

Kinny, P.D., Wijbrans, J.R., Froude, D.O., Williams, I.S., and Compston, W. (1990) Age constraints on the geological evolution of the Narryer Gneiss Complex, Western Australia. *Australian Journal of Earth Sciences* ***37*****(**1), 51-69.

Kramers, J.D. and Tolstikhin, I.N. (1997) Two terrestrial lead isotope paradoxes, forward transport modelling, core formation and the history of the continental crust. *Chemical Geology* **139**, 75-110.

Kramers, J., Frei, R., Newville, M., Kober, B. and Villa, I. (2009) On the valency state of radiogenic lead in zircon and its consequences. *Chemical Geology*, ***261*****,** 4-11.

Kusky, T.M. (1998) Tectonic setting and terrane accretion of the Archaean Zimbabwe craton. *Geology* **26**, 163-166.

Luais, B. and Hawkesworth, C.J. (1994) The generation of continental crust - an integrated study of crust-forming processes in the Archaean of Zimbabwe. *Journal of Petrology* **35**, 43-93.

Ludwig, K.R. (2001) Isoplot/Ex rev. 2.49. Berkeley Geochronology Centre, Special Publication 1a.

Mojzsis, S.J., Cates, N.L., Caro, G., Trail, D., Abramov, O., Guitreau, M., Blichert-Toft, J., Hopkins, M.D. and Bleeker, W. (2014) Component geochronology in the polyphase ca. 3920Ma Acasta Gneiss. *Geochimica et Cosmochimica Acta* **133**, 68-96.

Moorbath, S., Wilson, J.F., Goodwin, R. and Humm, M. (1977) Further Rb-Sr age and isotope data on early and late Archaean rocks from the Rhodesian Craton. *Precambrian Research* **5**, 229-239.

Wooden, J.L. and Mueller, P.A. (1988) Pb, Sr, and Nd isotopic compositions of a suite of Late Archean, igneous rocks, eastern Beartooth Mountains: implications for crust-mantle evolution. *Earth and Planetary Science Letters* ***87***, 59-72.

Mueller, P.A. and Wooden, J.L. (2012) Trace element and Lu-Hf systematics in Hadean-Archean detrital zircons: implications for crustal evolution. *The Journal of Geology* **120**, 15-29.

Næraa, T., Schersten, A., Rosing, M.T., Kemp, A.I.S., Hoffmann, J.E., Kokfelt, T.F. and Whitehouse, M.J. (2012) Hafnium isotope evidence for a transition in the dynamics of continental growth 3.2 Gyr ago. *Nature* **485**, 627-630.

Nägler, T.F., Kramers, J.D., Kamber, B.S., Frei, R. and Prendergast, M.D.A. (1997) Growth of subcontinental lithospheric mantle beneath Zimbabwe started at or before 3.8 Ga: Re-Os study on chromites. *Geology* **25,** 983-986.

Nemchin, A.A., Pidgeon, R.T. and Whitehouse, M.J. (2006) Re-evaluation of the origin and evolution of > 4.2 Ga zircons from the Jack Hills metasedimentary rocks. *Earth and Planetary Science Letters* **244**, 218-233.

Nutman, A.P., Bennett, V.C., Friend, C.R., Hidaka, H., Yi, K., Lee, S. R. and Kamiichi, T. (2013) The Itsaq Gneiss Complex of Greenland: Episodic 3900 to 3660 Ma juvenile crust formation and recycling in the 3660 to 3600 Ma Isukasian orogeny. *American Journal of Science* ***313***, 877-911.

Oberthür, T., Davis, D.W., Blenkinsop, T.G. and Hohndorf, A. (2002) Precise U-Pb mineral ages, Rb-Sr and Sm-Nd systematics for the Great Dyke, Zimbabwe - constraints on late Archean events in the Zimbabwe craton and Limpopo belt. *Precambrian Research* **113**, 293-305.

Oversby, V.M. (1975) Lead isotopic systematics and ages of Archaean acid intrusives in Kalgoorlie-Norseman area, Western Australia. *Geochimica et Cosmochimica Acta* **39**, 1107-1125.

Pietranik, A.B., Hawkesworth, C.J., Storey, C.D., Kemp, A.I.S., Sircombe, K.N., Whitehouse, M.J. and Bleeker, W. (2008) Episodic, mafic crust formation from 4.5 to 2.8 Ga: New evidence from detrital zircons, Slave craton, Canada. *Geology* **36**, 875-878.

Prendergast, M. D. and Wingate, M. T. D. (2013) Zircon geochronology of late Archean komatiitic sills and their felsic country rocks, south-central Zimbabwe: A revised age for the Reliance komatiitic event and its implications. *Precambrian Research* **229**, 105-124.

Reimink, J.R., Davies, J.H.F.L., Chacko, T., Stern, R.A., Heaman, L.M., Sarkar, C., Schaltegger, U., Creaser, R.A. and Pearson, D.G. (2016) No evidence for Hadean continental crust within Earth's oldest evolved rock unit. Nature Geoscience **9,** 777-780.

Robertson, I.D.M. (1976) The geology of the country around Battlefields, Gatooma District. *Rhodesian Geological Survey Bulletin* **76**, 258.

Salje, E.K.H., Chrosch, J. and Ewing, R.C. (1999) Is "metamictization" of zircon a phase transition? *American Mineralogist* **84**, 1107-1116.

Scherer, E.E., Münker, C. and Mezger, K. (2001) Calibration of the Lutetium-Hafnium clock. *Science* **293**, 683-687.

Smirnov A.V., Evans D. D, Ernst R.E., Soderlund, U. and Li Z.X. (2013) Trading partners: Tectonic ancestry of southern Africa and western Australia, in Archean supercratons Vaalbara and Zimgarn. *Precambrian Research* **224**, 11-22.

Smith, C.B., Pearson, D.G., Bulanova, G.P., Beard, A.D., Carlson, R.W., Witting, N., Sims, K., Chimuka, L., and Muchemwa, E. (2009) Extremely depleted lithospheric mantle and diamonds beneath the southern Zimbabwe Craton. *Lithos* **112S**, 1120-1132.

Söderlund, U., Patchett, P.J., Vervoort, J.D. and Isachsen, C.E. (2004) The Lu-176 decay constant determined by Lu-Hf and U-Pb isotope systematics of Precambrian mafic intrusions. *Earth and Planetary Science Letters* **219**, 311-324.

Söderlund, U., Hofmann, A., Klausen, M.B., Olsson, J.R., Ernst, R.E., and Persson, P. O. (2010) Towards a complete magmatic barcode for the Zimbabwe craton: Baddeleyite U–Pb dating of regional dolerite dyke swarms and sill complexes. *Precambrian Research* **183**, 388-398.

Stacey, J.S. and Kramers, J.D. (1975) Approximation of terrestrial lead isotope evolution by a two-stage model. *Earth and planetary science letters* ***26*****,** 207-221.

Stern, R.A. and Bleeker, W. (1998) Age of the world's oldest rocks refined using Canada's SHRIMP: The Acasta Gneiss Complex, Northwest Territories, Canada. *Geoscience Canada*, **25**.

Stein, M. and Hofmann, A.W. (1994) Mantle plumes and episodic crustal growth. *Nature* **372,** 63-68.

Taylor, P.N., Kramers, J.D., Moorbath, S., Wilson, J.F., Orpen, J.L. and Martin, A. (1991) Pb/Pb, Sm-Nd and Rb-Sr geochronology in the Archean craton of Zimbabwe. *Chemical Geology* (Isotope Geoscience Section) **87**, 175-196.

Valley, J.W., Chiarenzelli, J.R. and McLelland, J.M. (1994) Oxygen isotope geochemistry of zircon. *Earth and Planetary Science Letters* **126**, 187-206.

Vervoort, J., Kemp, A., Fisher, C. M. (2012) No signficant production of continental crust pior to 3.8 Ga. Abstract TB11B-2570, AGU Fall meeting 2012, San Francisco.

Vervoort, J., Kemp, A., Fisher, C., Bauer, A. and Bowring, S. (2015) The Rock Record Has It About Right—No Significant Continental Crust Formation Prior to 3.8 Ga. Abstract V43D-05, AGU Fall meeting 2015, San Francisco.

Vervoort, J.D. and Kemp, A.I. (2016) Clarifying the zircon Hf isotope record of crust–mantle evolution. *Chemical Geology* **425,** 65-75.

Whitehouse, M.J. and Kamber, B.S. (2005) Assigning dates to thin gneissic veins in high-grade metamorphic terranes: A cautionary tale from Akilia, southwest Greenland. *Journal of Petrology* **46**, 291-318.

Wilde, S.A., Valley, J.W., Peck, W.H., and Graham, C.M. (2001) Evidence from detrital zircons for the existence of continental crust and oceans on the Earth 4.4 Gyr ago. Nature **409** (6817), 175-178.

Wilson, J.F. (1968) The geology of the country around Mashaba. *Rhodesia Geological Survey Bulletin* **62**.

Wilson, J.F. (1979) A preliminary appraisal of the Rhodesian Basement Complex. *Geological Society of South Africa*, Special Edition **5**, 1-23.

Wilson, J.F. (1990) A craton and its cracks - some of the behaviour of the Zimbabwe block from the Late Archean to the Mesozoic in response to horizontal movements, and the significance of some of its mafic dyke fracture patterns. *Journal of African Earth Sciences* **10**, 483-501.

Wilson, J.F., Nesbitt, R.W. and Fanning, C.M. (1995) Zircon geochronology of Archaean felsic sequences in the Zimbabwe craton: A revision of greenstone stratigraphy and a model for crustal growth, In Early Precambrian processes (eds. P.M. Coward and A.C. Ries) *Geological Society of London Special Publications*, pp. 109-126.

Wyche, S., Nelson, D.R. and Riganti, A. (2004) 4350–3130 Ma detrital zircons in the Southern Cross Granite–Greenstone Terrane, Western Australia: implications for the early evolution of the Yilgarn Craton. *Australian journal of Earth sciences* **51**, 31-45.

Zeh, A., Gerdes, A., Klemd, R. and Barton, J.M. (2008) U-Pb and Lu-Hf isotope record of detrital zircon grains from the Limpopo Belt - Evidence for crustal recycling at the Hadean to early-Archean transition. *Geochimica Et Cosmochimica Acta* **72**, 5304-5329.

Zeh, A., Gerdes, A. and Heubeck, C. (2013) U-Pb and Hf isotope data of detrital zircons from the Barberton Greenstone Belt: constraints on provenance and Archaean crustal evolution. *Journal of the Geological Society* **170**, 215-223.

Zeh, A., Stern, R.A. and Gerdes, A. (2014) The oldest zircons of Africa—Their U–Pb–Hf–O isotope and trace element systematics, and implications for Hadean to Archean crust–mantle evolution. *Precambrian Research **241***, 203-230.

Table 1: Summary of isotopic data for detrital zircon from the Zimbabwe Craton

Sample	Greenstone Belt	Group	Formation	lithology	no of concordant/ discordant data	youngest/ oldest concordant age (Ma)	range in εHf (<10 % discordance)	range in $\delta^{18}O$ (<10 % discordance)	range in Th/U (<10 % discordance)
BUC1	Buhwa	Belingwean/Lower Bulawayan	Buhwa	quarzite	17/10	3109/3593	(-5.0) - (+1.0)	(1.7) - (7.6)	(0.1) - (1.3)
Z12-1	Midlands	Upper Bulawayan	Mafic	sandstone	6/33	3549/3582	(-1.9) - (+0.4)	(5.5) - (6.4)	(0.1) - (1.0)
Z12-2	Shurugwi	Upper Bulawayan	Wanderer	quartzite cobble	6/15	3317/3347	(-7.5) - (+2.4)	(5.6) - (6.2)	(0.3) - (1.0)
Z04-15	Shurugwi	Upper Bulawayan	Wanderer	conglomerate	3/17	3537/3697	(-2.9) - (-0.7)	(5.3) - (6.2)	(0.3) - (0.5)
Z10-3	Njiri	Sebakwian		fuchsitic quarzite	30/26	3135/3821	(-5.2) - (+1.3)	(5.0) - (10.0)	(0.2) - (1.2)
Z10-4	Njiri	Sebakwian		fuchsitic quarzite	6/32	3393/3645	(-4.8) - (+0.2)	(3.6) - (5.6)	(0.4) - (1.5)

Figure 1

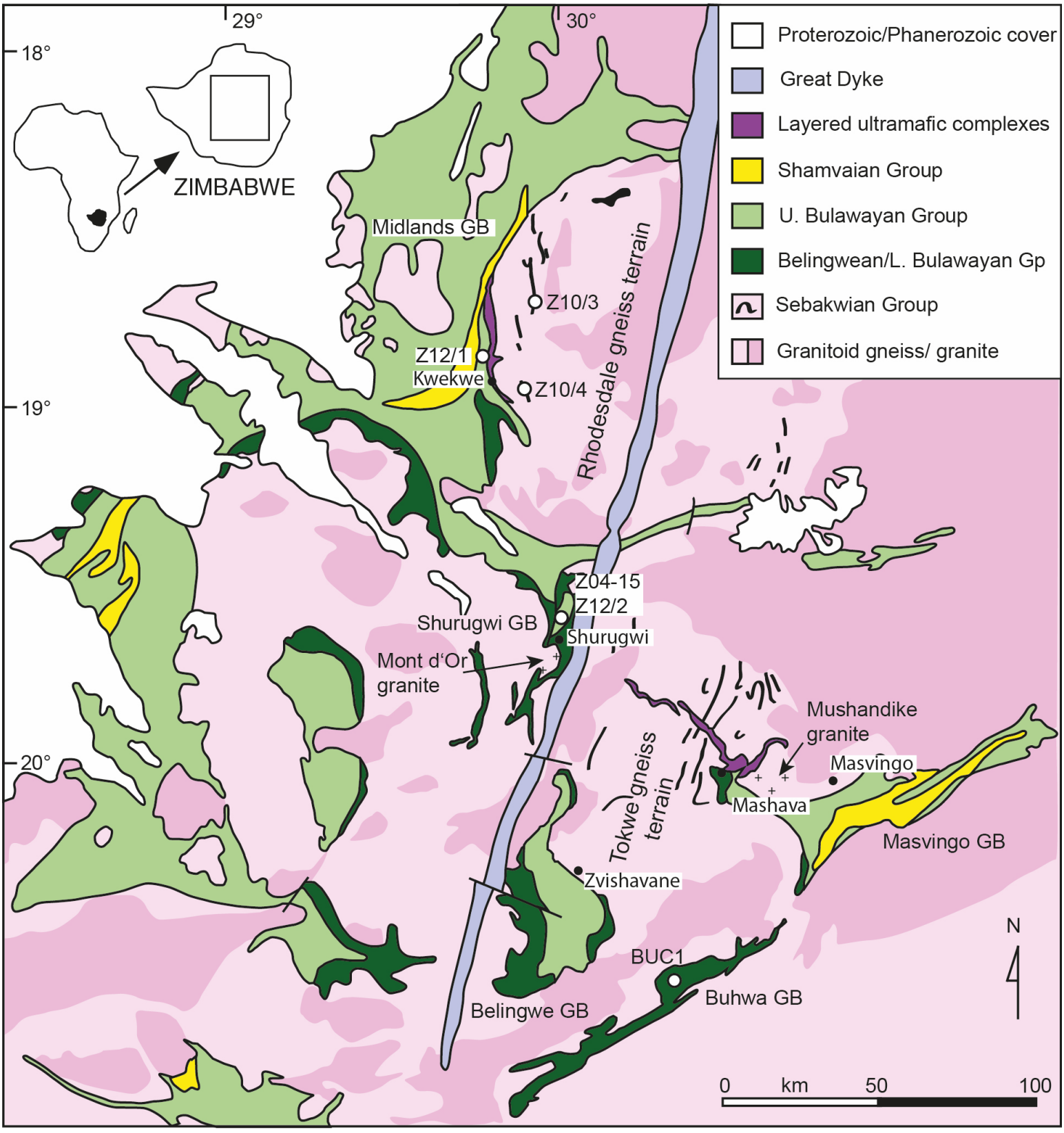

Figure 2

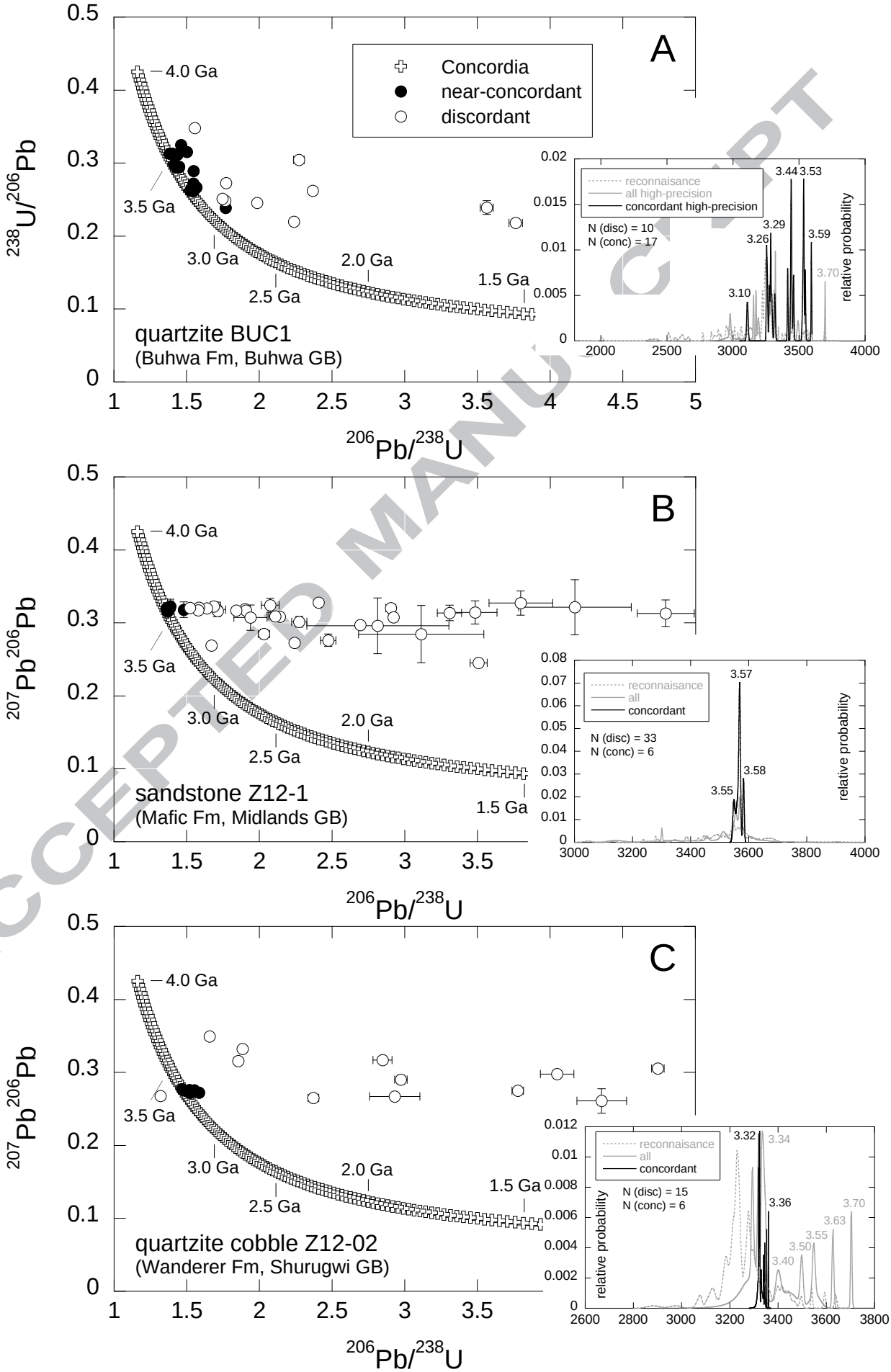

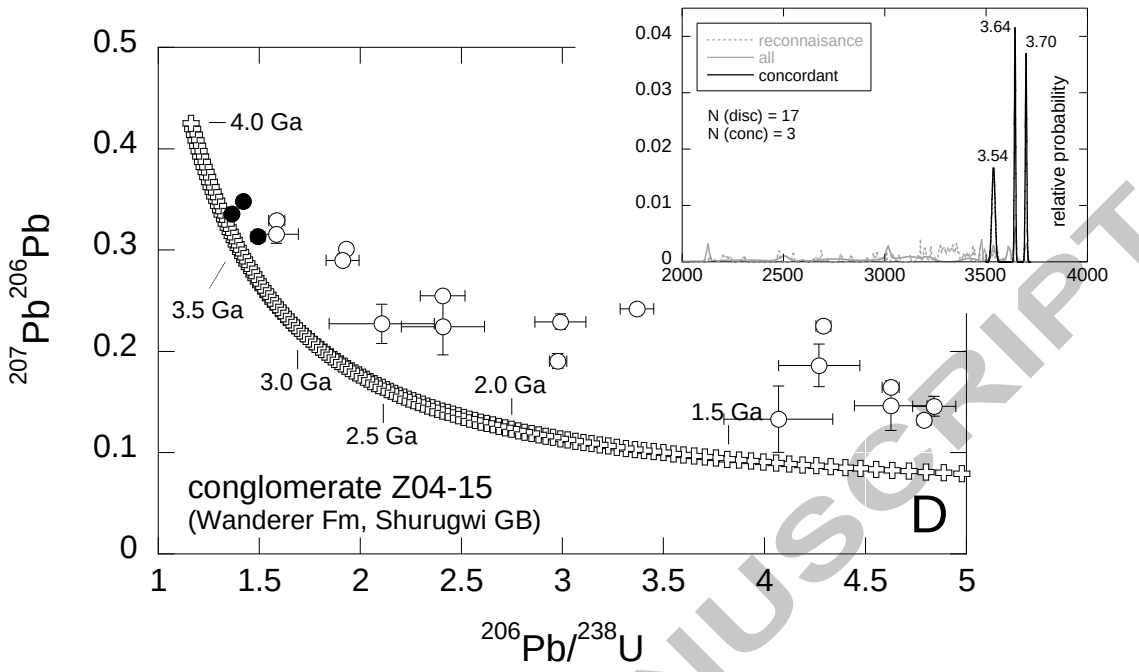

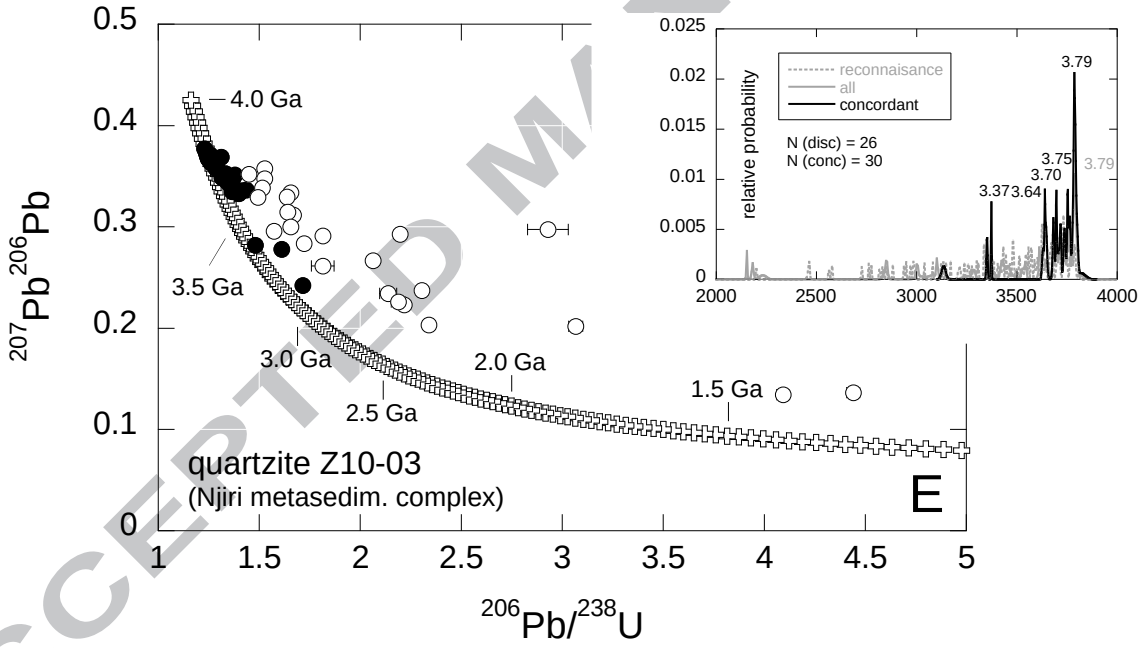

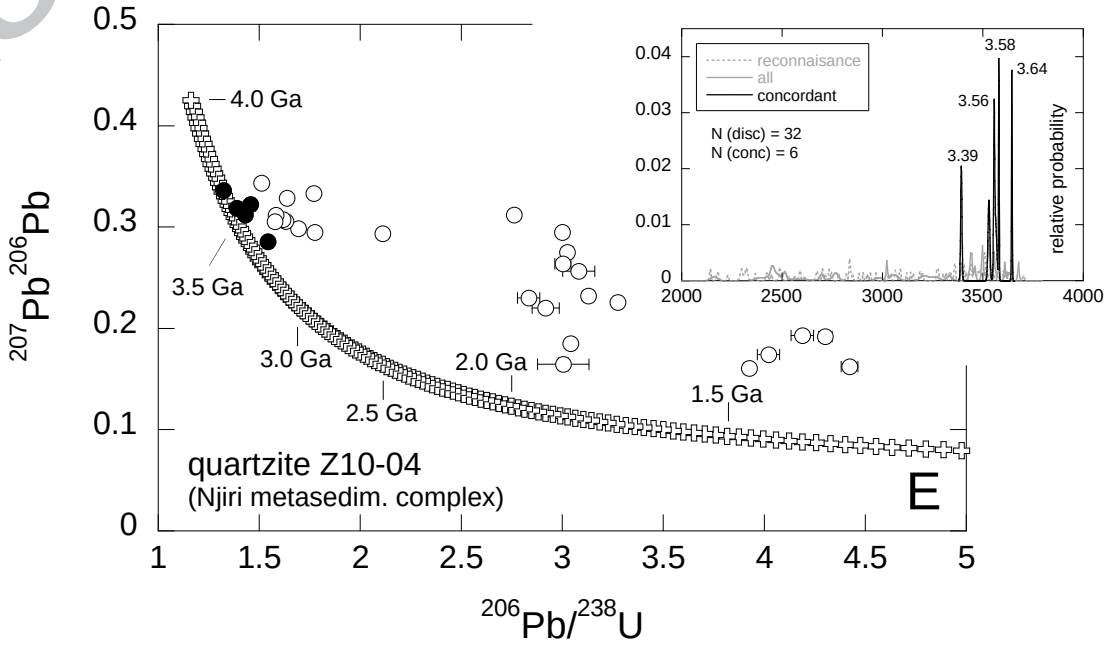

Figure 3

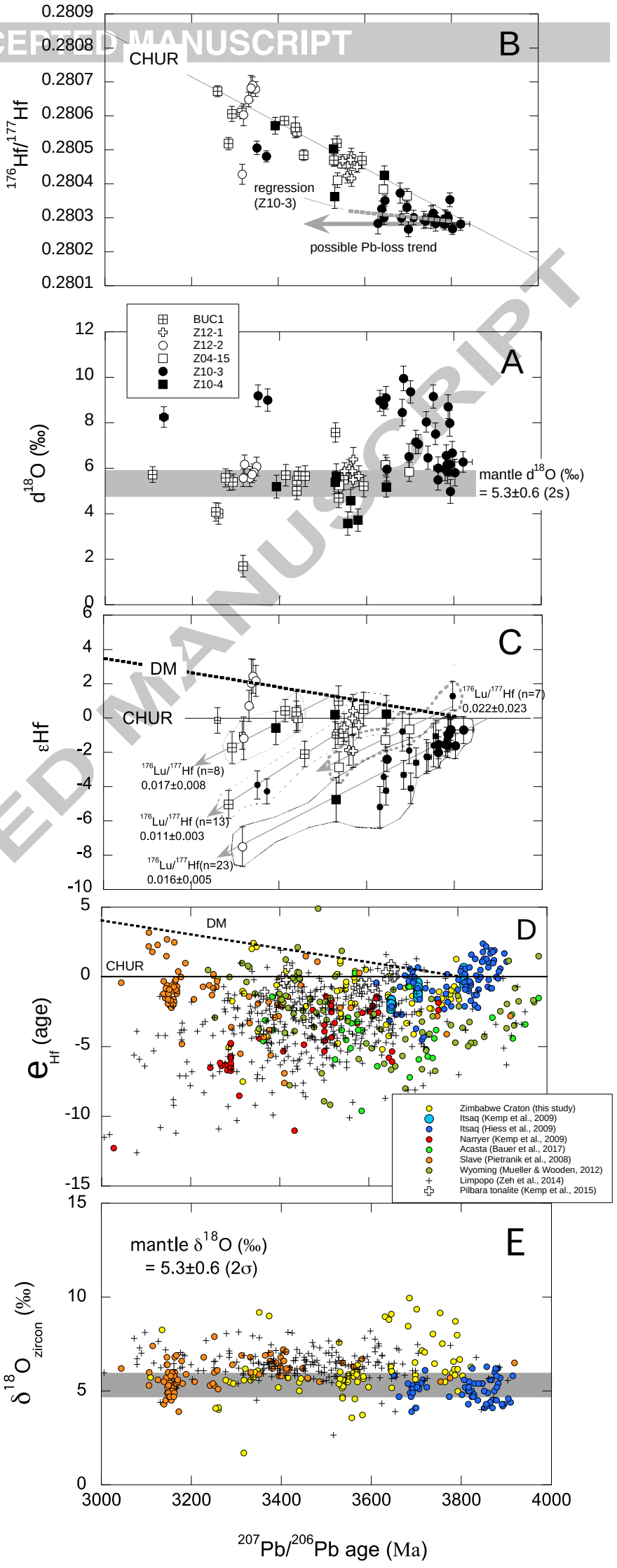

Figure 4

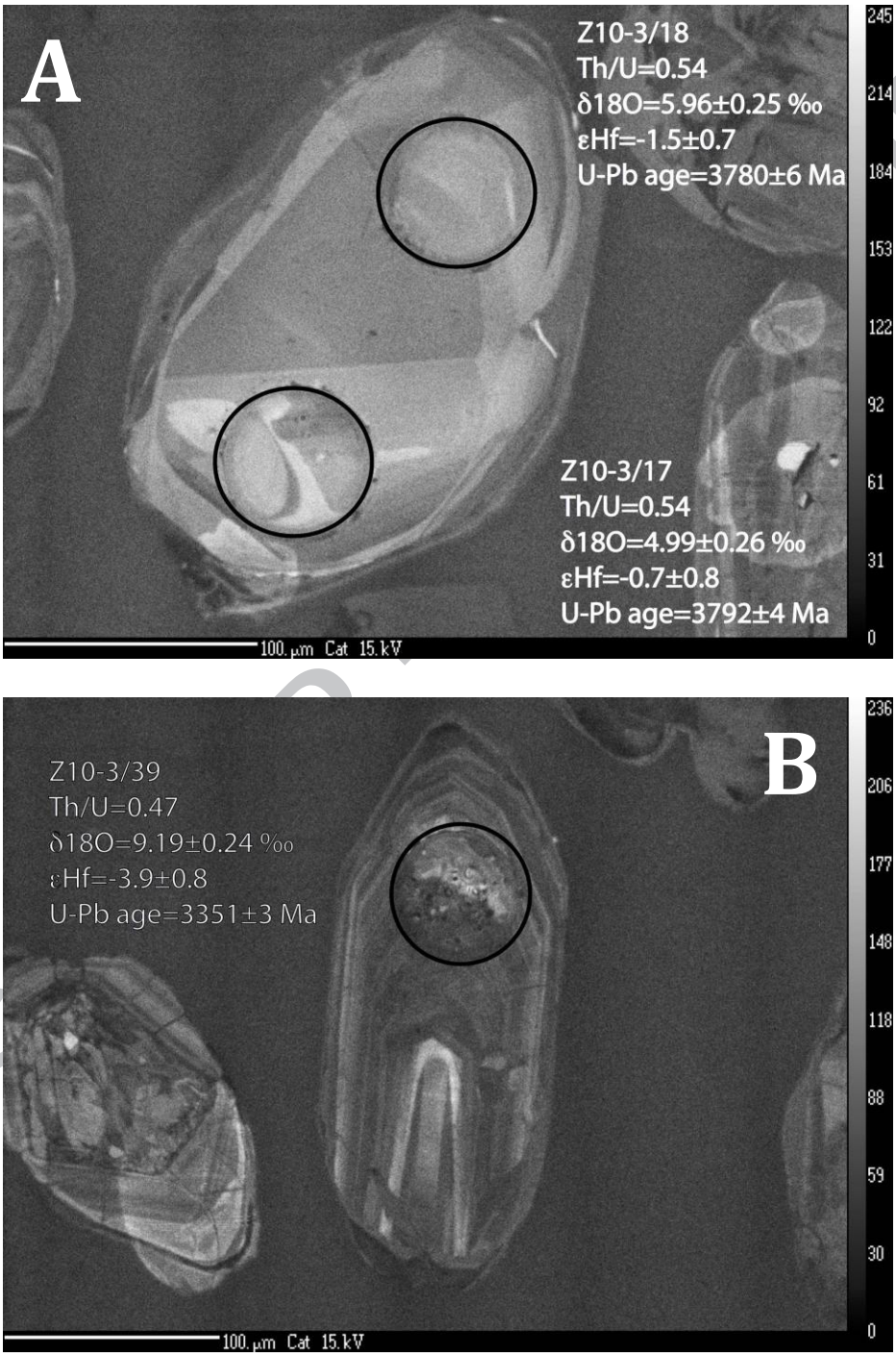

Figure 5